

Influences of variable thermal exposures on walking thermal comfort in hot summer by deeply studying the pedestrians' physio-psychological responses

Jianong Li, Jianlei Niu*, Cheuk Ming Mak

Department of Building Environment and Energy Engineering, The Hong Kong Polytechnic University, Hunghom, Kowloon, Hong Kong

Abstract

With more attentions of the walkability assessment considering thermal comfort, it is important to study walking thermal comfort in the complex urban continuums with variable microclimates. Thus, the heat exchange between a walking human body and its variable ambient was studied by measuring 70 subjects' surrounding meteorological parameters, skin temperatures, sweating, heart rates, and mixed thermal perceptions in two complex urban continuums. The extent of variable thermal exposures characterized by simultaneously varying wind and solar radiation during walking was described by the index Reverse Dynamic Thermal Environment (R_DTE), and its impacts were explored on physio-psychological responses. It is concluded that about 36% of produced heat is accumulated within 10 minutes' walking under variable thermal exposures with an air temperature over 28.0°C. The sweating rate is highly related to the R_DTE rather than the mean skin temperature deviation from the neutral one (ΔT_{sk}). An increased extent of variable thermal exposures significantly improves the thermal comfort as a walking person's skin wettedness (w) is over 0.4, whereas it causes discomfort when w is below 0.2. These findings can contribute to model walking thermal comfort and provide suggestions on creating comfort by adjusting variable thermal exposures in the urban continuums in hot days.

Key words: Walkability; Urban continuums; Heat exchange; The extent of variable thermal exposures; Sweating rate; Skin wettedness; Reverse Dynamic Thermal Environment

1. Introduction

Walking is a popular commuting mode and a healthy way to relax in daily life (Bravata et al., 2007). The built environment in the urban area is a significant determinant in integrating walking into citizens' daily routines (Kärmeniemi et al., 2018). However, a complex-built environment may trap solar radiation, block the wind, and cumulate anthropogenic heat, causing undesirable heat stress (Oleson et al., 2015), especially on hot days, which may hinder outdoor walking and make it much more uncomfortable due to a relatively high metabolic rate and notable sweating.

In view of this, neighborhood walkability assessments (Lo, 2009) begin to consider the outdoor walking thermal comfort. Labdaoui et al. (2021) developed a Street Walkability and Thermal Comfort Index (SWTCI) based on Physiological Equivalent Temperature (PET) at the street scale. Lee et al. (2020) explored the influence of PET and the Universal Thermal Climate Index (UTCI) on walking behavior in Hong Kong. It should be noted that the complex urban morphologies inherently lead to variable wind flow and solar radiation (Ouameur & Potvin, 2007), while walking in the urban continuums makes the human body exposed to different extents of variable microclimates, with the most noticeable simultaneously varying wind and solar radiation in different frequencies and rates (Li et al., 2022b). Meanwhile, variable thermal sensations have been reported when walking in the streets (Lau et al., 2019; Li et al., 2022b; Potvin, 2000; Vasilikou & Nikolopoulou, 2020), which indicates that the heat exchange between a human body and the urban environment is unstable. However, *PET* was developed for assessing outdoor thermal comfort under stable thermal conditions (Höppe, 1999; Höppe, 1993; Mayer & Höppe, 1987, Melnikov et al., 2018), and *UTCI* underestimated the impacts of changes in simultaneous solar radiation and wind conditions on outdoor thermal comfort (Li et al., 2022), even though it was developed for assessing thermal comfort under dynamic air temperatures and a relatively high metabolic rate (Bröde et al., 2009; Bröde et al., 2012; Fiala

et al., 2012). It seems that traditional thermal indices are inadequate to assess walking thermal comfort.

Therefore, an in-depth look at walking thermal comfort and its modelling are urgently required, especially under variable thermal exposures where the wind and solar radiation simultaneously vary. However, in the recent studies, many of them mainly focus on the impacts of walking speed (Zhang et al., 2020; Jia et al., 2022; Liu et al., 2020) and ambient air velocity (Jia et al., 2022) on walking thermal comfort in either environment chambers or semi-open places where the solar radiation is weak. They did not consider the impacts of variable wind and variable solar radiation at different extents caused by walking and complex building environments, which should not be neglected when assessing the walking thermal comfort in complex urban continuums.

Meanwhile, few studies measured sweating rate which is very common during walking because of the relatively high metabolic rate and a hot and humid thermal condition (Candas et al., 1983; Mitchell et al., 1976; Wang & Hu, 2018; Zhang et al., 2016). The sweating rate directly determines the evaporative heat loss, overall heat exchange, and the skin wettedness, which should be the key factor influencing walking thermal comfort. Under variable thermal exposures, it is possible that the sweating rate increases due to a heat gain from a rise in solar radiation but decreases due to the increased evaporative and convective heat loss caused by an increased wind speed, making the factors influencing the sweating rate different from those explored in the steady thermal conditions (Kraning & Sturgeon, 1983; Kubota et al., 1996; Kubota et al., 2004). Understanding the sweating rate is essential in exploring the heat exchange and physiological responses when walking under variable thermal conditions.

Our thermal comfort is theoretically predicted by physiological responses (Yao et al., 2008), while a change in thermal condition may cause “Alliesthesia” effects (De Dear et al., 2011; Liu

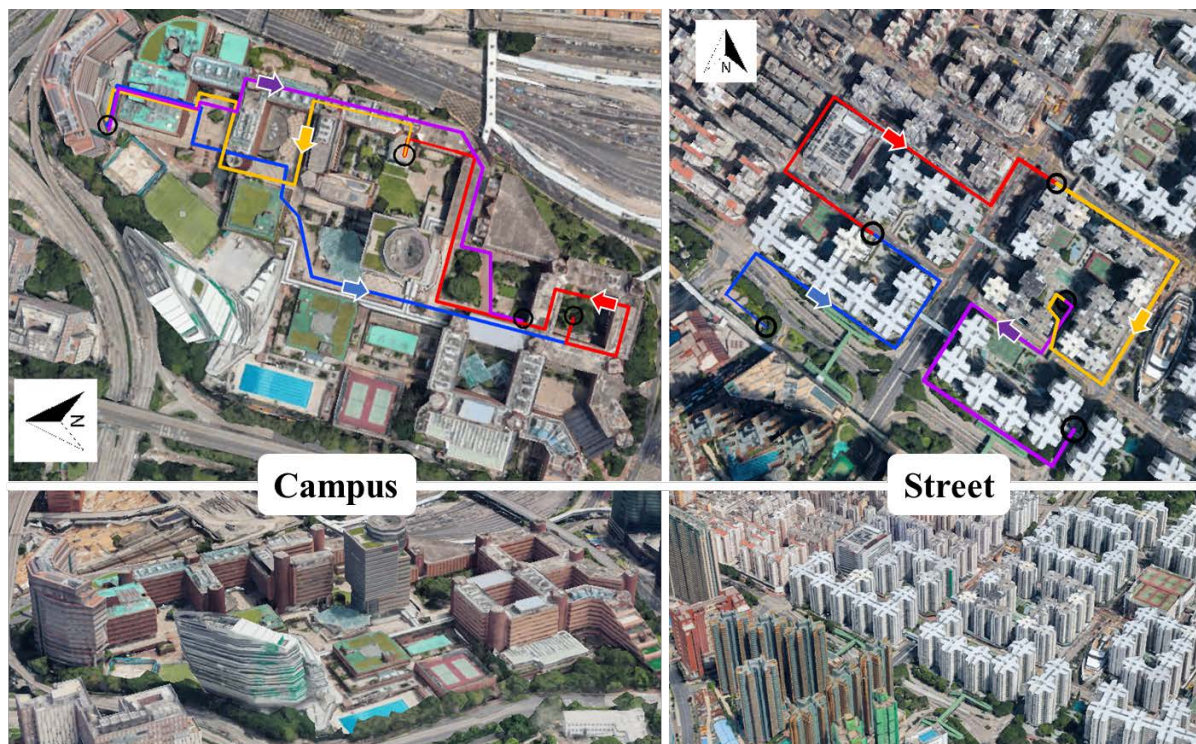
et al., 2020), producing the thermal comfort evaluations as an ‘overshoot’ that precedes physiological changes in the body (Arens et al., 2006). It is reported that the alliesthesia depends on the internal thermal state of the body (De Dear et al., 2011) and a strong thermal alliesthesia will occur when the body adaptation mechanisms are involved (e.g., sweating) (Liu et al., 2022). However, the alliesthesia is used to explain thermal comfort at the immediate point of change from one thermal exposure to another. Since walking and complex building environments cause constantly changing thermal exposures at different frequencies and rates, we know little about how the alliesthesia works on the overall thermal comfort under such conditions, as well as what the combined internal thermal state and extent of variable thermal exposures in a walking period can do to make the positive alliesthesia that brings comfort dominant. These knowledges are the foundations for evaluating walking thermal comfort and creating variable thermal exposures when designing sidewalks.

To fill the research gap and provide insights in modeling and improving walking thermal comfort in complex urban continuums, this study first reveals and studies the actual heat exchange between a walking person and his/her complex surroundings after measuring the sweat in a real scenario. Then, the factors influencing the sweating rate under variable thermal exposures are explored and compared with those found in steady indoor thermal environments. Last, the relationship between the physiological responses and walking thermal comfort is examined under different extents of variable thermal exposures. The results of the study have important reference values and can help with modeling walking thermal comfort, especially on hot days, as well as prompt the creation of variable thermal exposures on sidewalks to adjust walking thermal comfort.

2. Methodology

2.1 Experiment design

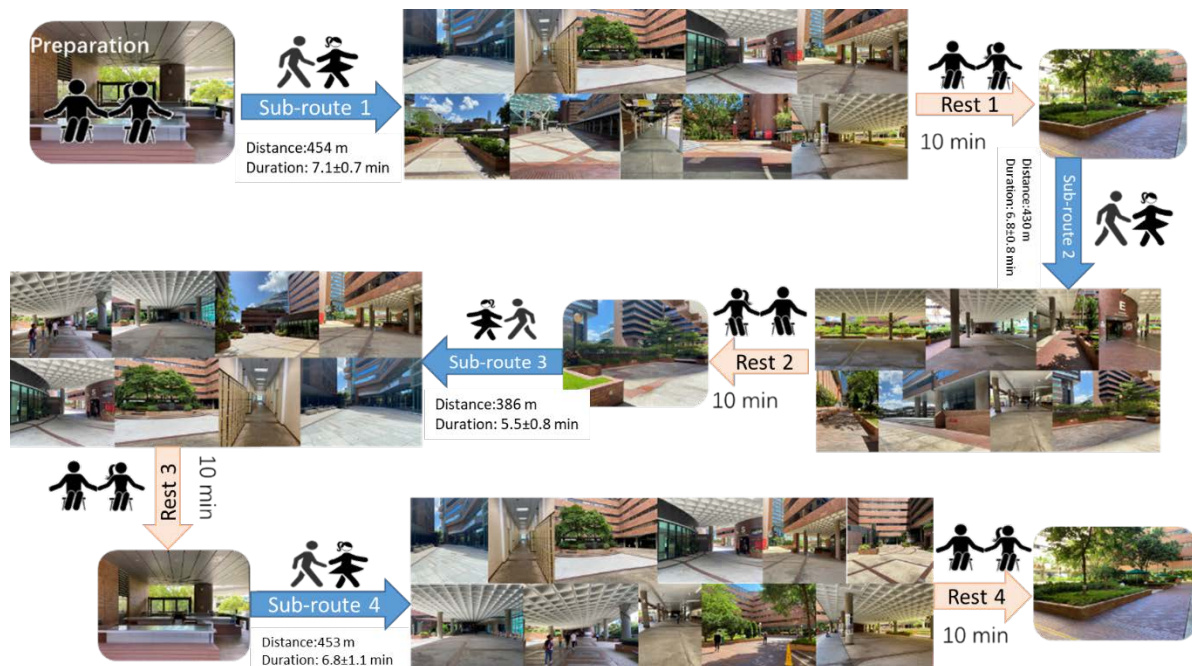
To achieve the objectives of the study, two urban areas with different morphologies: one university campus and one consisted of urban streets, were selected to conduct experiments from late July to early October 2020 in Hong Kong. Figure 1 shows the two areas and walking routes with a variety of urban morphologies and outdoor spaces, and the rich and variable thermal exposures can be achieved when walking. As shown in Figure 1, four sub-routes in each area were selected for experiments, with each sub-route being around 400 meters long to ensure the time spent on each sub-route under 10 minutes. The weather during the experiment period was regarded as summer season with an air temperature around 31.0 °C and a relative humidity around 75% (HKO, 2020), and experiment days in two areas had similar weather conditions.



Blue Line—Sub-route1 (walking period 1); Red Line—Sub-route2 (walking period 2); Yellow Line—Sub-route3 (walking period 3); Purple Line—Sub-route4 (walking period 4)

Figure 1. Walking routes on campus and in the urban streets: the colorful arrow representing the walking direction on each sub-route, and the black circle representing the rest place at the end of each sub-route.

70 college students (32 males and 38 females) were recruited as subjects in this study. Their ages are between 21 and 30 and their weight and heights are in the average level (Yang et al., 2005). The procedure of experiments is shown in Figure 2. For each experiment, one or two subjects were required to complete the following two stages: the preparation stage 1, in which subjects sat on a chair in a shaded area for 30 minutes for preparing the experiments and adapting to the outdoor thermal environments; and the walking stage 2, in which subjects walked from sub-route 1 to sub-route 4 in order and rested for 10 minutes at the end of each sub-route. It should be noted that in one experiment, one subject should finish walking on four sub-routes and resting four times. During walking, subjects will be exposed to variable microclimates and asked about their transient thermal perceptions to changes in solar radiation and wind speed.



a)



b)

Figure 2. Subjects' activities on a) a campus and in b) urban streets.

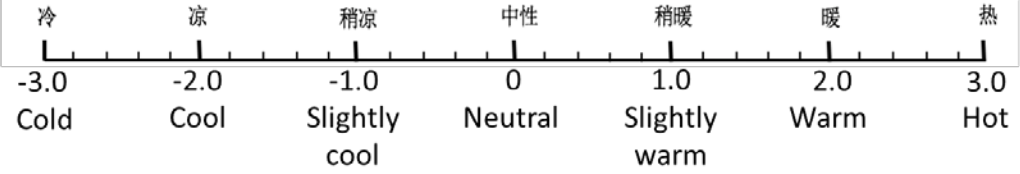
Each walking period varies due to the uneasily controlled walking speed, whereas the duration of the stage 2 was controlled within 90 mins. The subjects were asked to sit during rest and the resting places were all shaded areas. Besides, subjects worn short-sleeved T-shirts, short trousers, and sports shoes with a general clothing insulation of 0.3-0.4 clo during the experiments. The experiment date and initial thermal conditions at stage 1, as well as the characteristics of two experiment areas are summarized in Table 1. The similar initial thermal conditions in Stage 1 were to ascertain that the subjects were in the similar thermal states before engaging in walking.

Table 1 Experiment dates, daily air temperatures, and initial thermal conditions at stage 1 on campus and in the urban street

Experiment Area	Experiment time	Experiment date	Daily Air temperature (min-max)	Initial thermal condition at stage 1			
				T_a (°C)	RH (%)	T_g (°C)	v (m/s)
Campus Less Crowded Noise Decibel: 64dBA Building density (0.34) Green density (0.13)	AM10:00- 12:00	7/21	28.1-34.7	29.4	64.8	29.7	1.2
		7/29	28.6-34.9	29.3	73.8	30.6	1.4
		8/8	28.4-34.4	30.3	67.5	30.5	1.3
		8/15	27.9-33.0	29.2	70.1	30.1	1.0
		8/18	25.6-29.9	28.5	73.2	29.7	1.2
		9/12	26.2-32.4	30.7	69.0	32.2	1.6
		9/21	25.5-29.7	28.6	81.1	28.8	1.5
		9/22	26.6-31.4	29.0	73.0	29.9	1.0
		9/24	27.1-31.3	27.8	76.1	29.2	1.2
		9/25	26.6-31.4	28.4	69.8	28.7	0.9
	PM 14:30- 16:30	9/26	27.1-29.7	28.1	72.8	28.7	1.4
		7/27	28.4-33.5	30.9	63.7	30.9	0.5
		7/29	28.6-34.9	31.8	65.4	32.6	0.9
		7/30	26.0-34.9	30.7	64.8	30.7	1.1
		8/5	26.0-34.9	29.8	76.4	29.9	1.1
		8/8	28.4-34.4	31.9	65.0	33.1	1.4
		8/10	28.3-33.0	30.1	68.4	30.5	1.2
		8/20	27.2-32.2	28.4	73.0	30.5	1.1
		9/18	26.4-30.2	29.0	71.2	30.2	1.8
		9/23	27.4-31.9	30.1	69.3	31.0	1.1
Urban streets Crowded Noise Decibel: 68dBA Building density (0.49) Green density (0.02)	AM10:00- 12:00	9/26	27.1-29.7	28.5	69.0	28.8	1.1
		10/3	26.7-31.9	29.6	62.0	30.6	1.6
		8/28	25.0-34.2	30.9	72.0	32.6	0.6
		9/4	28.2-34.3	30.2	76.0	31.3	0.6
		9/16	27.3-32.9	30.5	75.3	31.3	0.4
		9/23	27.4-31.9	30.1	68.6	32.1	0.9
		9/26	26.2-29.4	28.3	75.0	30.5	1.8
		10/3	26.7-31.9	28.7	69.8	30.6	1.4
	PM 14:30- 17:00	10/4	26.8-31.4	29.9	66.4	32.4	0.8
		8/22	27.2-33.3	31.9	61.8	33.5	0.8
		8/29	27.8-33.2	31.4	68.9	32.5	0.7
		8/31	28.2-34.3	31.0	64.3	31.0	1.0
		9/5	25.2-30.6	30.5	68.0	33.0	0.5
		9/6	27.2-32.3	30.1	72.9	32.5	0.7
		9/7	26.8-33.3	31.1	70.5	33.4	1.2
		9/16	27.3-32.9	31.1	72.1	32.6	1.2
		9/22	26.6-31.4	30.2	69.0	32.6	0.9
		9/24	27.1-31.3	29.9	73.9	30.4	1.2

The transient thermal perceptions that subjects needed to report during walking include ASHRAE 7-point Thermal Sensation Vote (*TSV*) and Thermal pleasure adjustment (*TP*) and the questions are shown as Figure 3a. During walking, subjects were asked to answer these two questions as long as encountering changes in sunlight, shade, and wind to record their transient

perceptions through an artificial intelligence (AI) recorder (Figure 3b). The questions are designed to identify if the variable thermal exposures cause pleasant or annoyed feelings in addition to traditional thermal sensation to understand the actual walking thermal comfort.

Questionnaire Survey				
<p>1. Thermal Sensation Vote (TSV)</p> <div style="text-align: center; margin: 10px 0;">  </div> <p>2. Thermal Pleasure vote (TP)</p> <table border="1" style="width: 100%; border-collapse: collapse; margin-top: 10px;"> <tr> <td style="width: 33%; text-align: center; padding: 5px;">1—Hot-biased annoyance</td> <td style="width: 33%; text-align: center; padding: 5px;">2— It's okay</td> <td style="width: 33%; text-align: center; padding: 5px;">3— Cool-biased pleasure</td> </tr> </table>		1—Hot-biased annoyance	2— It's okay	3— Cool-biased pleasure
1—Hot-biased annoyance	2— It's okay	3— Cool-biased pleasure		

a)



b)

Figure 3 On-site survey: a) Questions to be answered during walking; b) AI recorder and transcription software to record transient thermal perceptions (Li et al., 2022b).

2.2 Physical and physiological measurements

2.2.1 Meteorological variables

In order to measure the ambient environment around a walking people, a movable weather station mounted on a baby carriage was used, which is shown as Figure 4. To reduce the

possible measurement error during movement, the station is protected by the shock-absorber of the baby carriage and wheeled gently and steadily during the experiments. In each experiment, this cute movable weather station was wheeled by a project assistant, walking alongside subjects at a consistent space to measure surrounding meteorological parameters including air temperature (T_a), wind speed (v), relative humidity (RH), and black globe temperature (T_g) at pedestrian level. The data were collected by the equipment at a 1s interval, and the specification of each equipment is displayed in Table 2.

It should be noted that the wind measured in this study considers the air disturbance caused by walking, representing the real wind felt by a walking people. The mean radiant temperature (T_{mrt}) was used in this study to reflect the solar radiation received by the subjects during walking, and T_{mrt} was calculated from the measured T_g using Eq. 1 and then adjusted to the T_{mrt} calculated from 6 direction irradiation by Kipp & Zonen CNR4 net radiometers using Eq. 2 (Li et al., 2022b) to guarantee the accuracy. Due to the response time required by the black ball thermometer when reading T_g , the measured value of T_g after each upward or downward change in solar radiation was adjusted using the method displayed in the Appendix C. The system time of all instruments were calibrated with local time before experiment to ensure that the transient environmental parameters were matched well with the recorded TSV of the subjects.

$$T_{mrt(T_g)} = \left[(T_g' + 273.15)^4 + \frac{1.10 \times 10^8 \times v^{0.6} \times (T_g - T_a)}{\varepsilon D^{0.4}} \right]^{1/4} - 273.15 \quad (1)$$

where, T_g' is the calibrated T_g ; D of 75 mm is the black globe diameter; the emissivity (ε) of the globe was set to 0.95 for a typical black globe sensor.

$$T_{mrt(T_g')} = 1.1383 \times T_{mrt(6-direction)} - 3.6986 \quad (2)$$

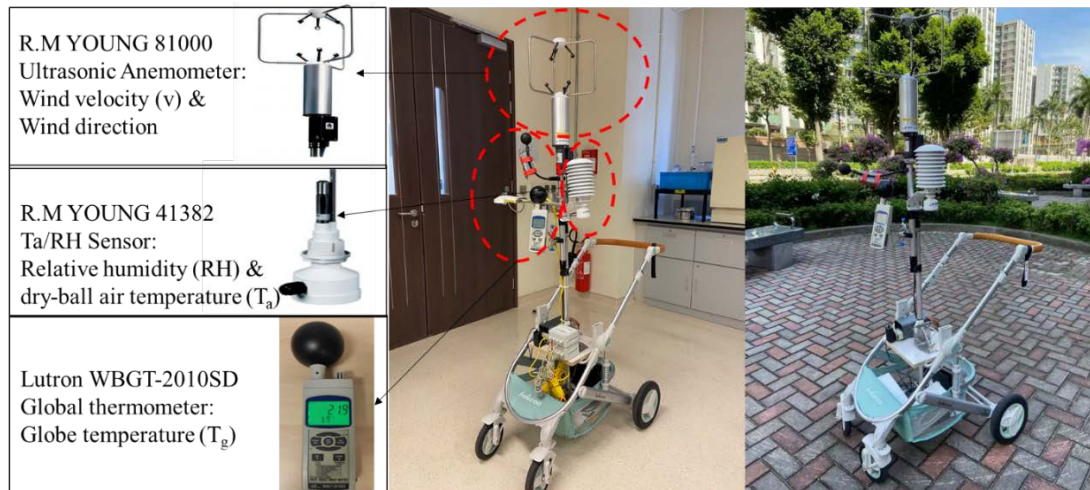


Figure 4 Movable mini weather station

Table 2 Equipment specifications

Meteorological parameter	Instrument	Measuring Range	Accuracy
Air temperature	R.M.YOUNG 41382	-50-50 °C	±0.3 °C
Relative humidity		0-100%	±1%
Wind speed	R.M.YOUNG 81000	0-40 m/s	±0.05 m/s
Globe temperature	Lutron WBGT-2010SD	0-80 °C	±0.6 °C

2.2.2 Physiological variables

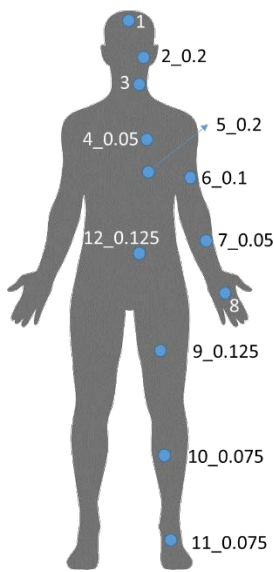
1) Local skin temperature and heart rate

The skin temperatures of 12 body points were measured with small and portable thermocouples named i-Button temperature sensors during movement (Figure 5a). The information of the i-Button is presented in Figure 5b. The sensors were closely adhered to the skin surface with medical adhesive tape to reduce contact surface space. The measured skin temperatures were automatically recorded to the i-Button for each 3s. All i-Button temperature recorders were calibrated against a standard mercury thermometer with an accuracy of 0.1 °C before measurement. 9 points local skin temperatures including the cheek's skin temperature

were used to determine the mean skin temperature using Houdas and Colin's method (Houdas & Ring, 2013) as shown in Eq. (3) and the weighting factors of these 9 points are shown in Figure 5a. In addition to the measurement of skin temperature, subjects were required to wear a Polar Verity Sense (Figure 5c) on the left upper arm to record their heart rate during walking.

$$T_{sk,m} = \sum_{i=1}^9 k_i T_i \quad (3)$$

where T_i is local skin temperature, k_i is the corresponding weighting factor.



a)



b)



c)

Figure 5 Measured local skin temperatures: a) Measurement sites and corresponded weighting factor. 1 forehead, 2 face, 3 neck, 4 cheek, 5 back, 6 right upper arm, 7 right forearm, 8 hand, 9 anterior thigh, 10 anterior calf, 11 right foot, 12 abdomen; b) Thermocouples (i-Button) for measuring skin temperatures; c) Polar Verity Sense for recording heart rate.

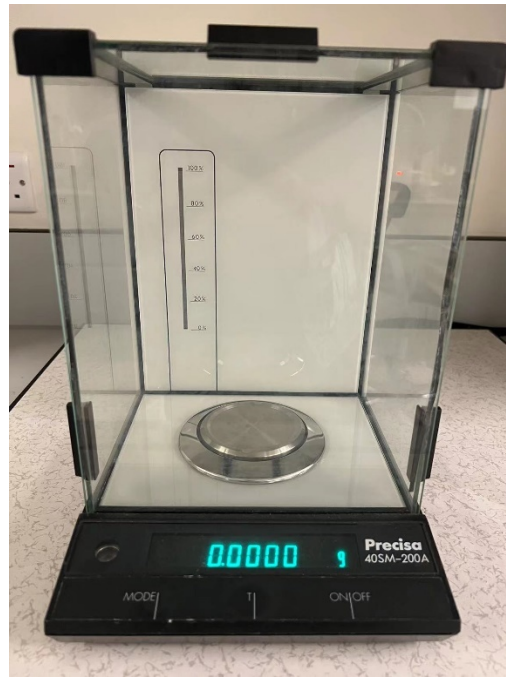
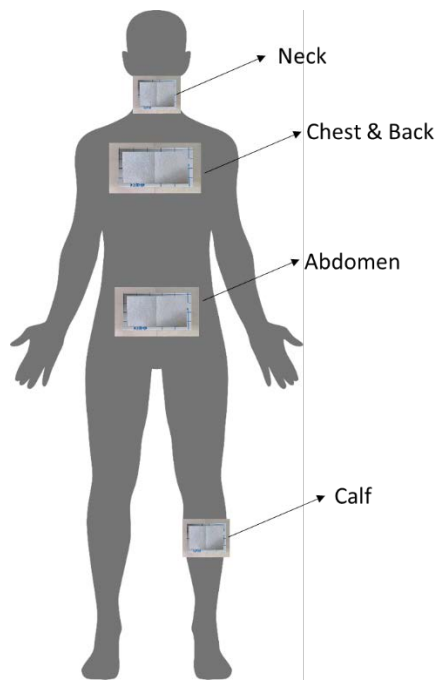
2) Local sweating rate (LSR)

The technical absorbent (TA) method was applied for measuring local sweat in this study. The TA method used patches of highly absorbent material of a fixed area and placed over the skin for a short period time to estimate a snapshot of local sweat rate across larger skin area (Havenith et al., 2008; Morris et al., 2013). The TA patches used in this study consisted of a large square patch (#7023 needle punch nonwoven fabric, Technical Absorbents, North East Lincolnshire, UK), gauze and adhesive film. Figure 6a shows the TA patch with a middle square patch (118.8 cm²) and a 1.0-cm-wide border sponge tape. The sponge tape was used to fix the gauze to the absorbent fiber and keep it from absorbing the sweat from surrounding area. To prevent the TA patch from slipping during sweating, an adhesive film with high air permeability was used. In each experiment, subjects were tested about their sweat rate in four walking periods.

Five major body parts that secrete sweat were selected to adhere TA patches (Figure 6b) (B. Li, 2012). It should be noted that the position of TA patch and that of i-Button should be separated. Prior to experiment, each TA patch was assembled by assistants using no powdered gloves in an experiment chamber with a constant relative humidity of 50%. Each TA patch was numbered and placed in its own separate impermeable plastic bag (Ziploc) before being weighed using an electronic balance with a readability of 0.0001g and an accuracy of ± 0.0001 g (Figure 6c). After weighing, all sealed plastic bags were stored in a box with constant air temperature of 24 °C and constant relative humidity of 50%. The size of patch for neck was half of that for other parts.



a)



b)

c)

Figure 6 Measurement of local sweating rate: a) Design of Technical Absorbent patches; b) Sites for collecting sweat (neck, chest, back, abdomen and calf); c) the high precision electronic balance

At preparation state and each rest state, the skin surface area of application was wiped completely dry using paper towel thirty seconds prior to the start of next walking to make sure the correct collection of the following sweat. The patches were then stuck to the skin areas. After finishing one walking period (less than 10 minutes), all patches were removed, and each patch was placed immediately into its original sealed bags. All TA patches used in the experiments were stored in a large impermeable plastic bag, and then reweighed in the chamber after finishing the whole experiment. The difference in post- and pre-experiment mass of an unused TA patch was calculated for each experiment to illustrate the error generated over lengthy period experiments. In most cases, the error was less than 0.3 mg, which can be neglected.

2.3 Calculation and indices

2.3.1 Heat exchange

In order to ensure the normal function of thermo-regulation, the heat balance (Eq. 4) inside the body should be satisfied.

$$M - W = R + C + E_{dif} + E_{sw} + C_{res} + E_{res} + S \quad (4)$$

where, M is the rate of metabolic rate production; W is the rate of mechanical work accomplished, which is assumed to be 0 in this study; E_{dif} is the evaporative heat loss of moisture diffused through the skin; E_{sw} is evaporative heat loss by sweat; C_{res} is convective heat loss from respiration; E_{res} is the evaporative heat loss from respiration; S is the heat storage.

The metabolic rate M in Eq. (5) is estimated from recorded heart rate HR_{wm} during walking (Malchaire et al., 2017), and the general formula is shown as the following. It reflects subjects' activity level as a result of varying stride length and stride frequency while walking. The determination of each parameter in the Eq. (5) can refer to the Appendix A.

$$M = \left(\frac{MWC - M_0}{HR_{max} - HR_0} (HR_{wm} - HR_0) + M_0 \right) / A_b \quad (5)$$

The sensible heat loss, including radiative heat loss R and convective heat loss C , was calculated by Eq. 6 with operative temperature T_o .

$$C + R = (MST - T_o) / (R_{cl} + \frac{1}{f_{cl}h}) \quad (6)$$

$$T_o = (h_r T_{mrt} + h_c T_a) / (h_r + h_c) \quad (7)$$

$$h_c = 9.93u^{0.54} \times (1 + 1.03 \times TI \times u^{0.5}) \quad (8)$$

The convective heat transfer coefficient h_c in this study takes into account the impacts of wind turbulence intensity on convective heat transfer (Yu et al., 2020). The calculation of each parameter in the Eqs. (6-8) can also refer to the Appendix A.

The total heat and moisture losses due to respiration consisted of evaporative heat loss from respiration E_{res} and convective heat loss from respiration C_{res} , and were calculated with the following Eqs. (9-10).

$$E_{res} = 0.0173M(5.87 - p_a) \quad W/m^2 \quad (9)$$

$$C_{res} = 0.0014M(MST - T_a) \quad W/m^2 \quad (10)$$

where T_a is the average air temperature in each walking period and p_a is corresponded water vapor pressure in ambient air, in kPa.

The evaporative heat loss of moisture diffused through the skin E_{dif} was calculated by Eq. (11) obtained from the ASHRAE handbook (ASHRAE, 2017) and related standards (ISO 2005).

$$E_{dif} = 3.05[5.73 - 0.007(M - W) - p_a] \quad (11)$$

The evaporative heat loss E_{sw} by sweat can be determined by a sweating rate which is calculated from on-site measurements. The total sweating rate $m_{sw_measured,j}$ of body in each walking period was calculated by Eq. (12), yielding values in $g \cdot cm^{-2} \cdot min^{-1}$ or $g \cdot m^{-2} \cdot h^{-1}$.

$$m_{sw_measured,j} = \frac{\sum_i^5 (m_{l,i-j} - m_{0,i-j})}{(S_{patch-neck} + 4 \times S_{patch-other parts}) \times T_{walking-j}} \quad (12)$$

where, m_0 and m_l are weights of each TA path before and after experiments; $i = 1, 2, 3, 4, 5$ means the number of body part; $j = 1, 2, 3, 4$ means the number of walking period; $T_{walking-j}$ presents the j^{th} walking period; $S_{patch-other parts}$ is equal to 118.8 cm^2 and $S_{patch-neck}$ is equal to 32.5 cm^2 ;

Sweating rate can be also predicted by the metabolic rate difference from rest metabolic rate ΔM and the mean skin temperature deviation from the neutral one Δt_{sk} using Eq. (13) which was developed in steady thermal environments (Kubota et al., 2004; Wang & Hu, 2018).

$$\dot{m}_{sw} = 0.63(\Delta M) + 50 \times \Delta T_{sk} \quad g/(m^2 \cdot h) \quad (13)$$

The calculation of ΔM and ΔT_{sk} can refer to the Appendix A.

Given the sweating rate, the proportion of sweat that is being evaporated (r_{ev}) should be known to determine E_{sw} using Eqs. 14-17.

$$E_{sw} = r_{ev} \cdot \dot{m}_{sw} \cdot h_{fg}/3600 \quad (14)$$

$$r_{ev} = 1 - \frac{w^2}{2} \quad (15)$$

$$w = \frac{E_{sw}}{E_{max}} \quad (16)$$

$$E_{max} = (h_c + h_r) \cdot i_m \cdot LR \cdot (p_{sk,s} - p_a) \quad (17)$$

Eq. (15) indicated that r_{ev} will be 0.955 and secreted sweat can be evaporated efficiently even skin wettedness reaches to the upper limits of comfort ($w = 0.3$) (Gagge et al., 1969). The h_{fg} of 2430kJ/kg is the latent heat of water vaporization at 30°C. Therefore, the following equation (18) should be satisfied to determine the w in each walking period.

$$\frac{(1 - \frac{w_d^2}{2}) \cdot \dot{m}_{sw_{measured}} \cdot h_{fg}/3600}{E_{max}} = w_d \quad (18)$$

The solution w_d of Eq. (18) rounded to 0.01 is thus the final w , which is used to calculate actual E_{sw} and heat storage S . It should be noted that the calculated E_{sw} with a calculated w_d using Eq. 16 is supposed to be lower than the required E_{sw} for satisfying the heat balance equation (4) given the other heat losses, otherwise the w_d was wrong, which might be caused

by wrong calculated sweating rate from on-site measurements. In view of this, w_d is also a method to examine if the sweat collected during experiments is correct.

2.3.2 Mixed Perception Index and Reverse Dynamic Thermal Environment

As mentioned in the introduction, walking thermal comfort is complex and easily affected by the thermal environmental stimulation. The mixed perception index (MP) developed by Li et al. (2022b) was used to accurately describe walking thermal comfort under variable thermal exposures. MP reflects both thermal sensation and thermal pleasure during walking (Figure 3a), and it is defined as the ratio of normalized transient thermal sensation vote ($nTSVt$) to transient thermal pleasure vote (TPt), as shown in Eq. (18).

$$MP = \frac{nTSVt}{TPt} \quad (18)$$

The MP scale runs is from 0 to 1, with MP values ranging from 0.1 to 0.3 indicating comfort-biased thermal states with TSV from -1 (slightly cool) to 3 (hot) but TP of 1 or 2 (pleasant or neither pleasant nor annoying feeling); values ranging from 0.4 to 0.5 indicating warm-but-acceptable thermal states with TSV from 1 (slightly warm) to 3 (hot) but TP of 2 (neither pleasant nor annoying feeling), and values over 0.5 indicating discomfort-biased thermal states with TSV over 0 (neutral) and TP of 3 (annoying feeling).

To study how variable thermal exposures influence the physio-psychological responses during walking, the variable thermal exposures characterized by notably varying wind and solar radiation needs to be defined and quantified. Therefore, the Reverse Dynamic Thermal Environment index (R_DTE) was used, which quantifies and grades the intensity of simultaneous variations in wind and solar radiation experienced while walking outdoors (Li et al. 2022b). R_DTE was derived based on the mean skin temperature variability within a short period (<10 mins) which can be predicted by the magnitudes, change rates, and variation frequency of wind and solar radiation in this time period. R_DTE is then calculated by Eq. (19).

$$R_DTE = 6.356 - 0.043 \times SVI_{mrt} - 0.013 \times SVI_v - 0.091 \times T_a \quad (19)$$

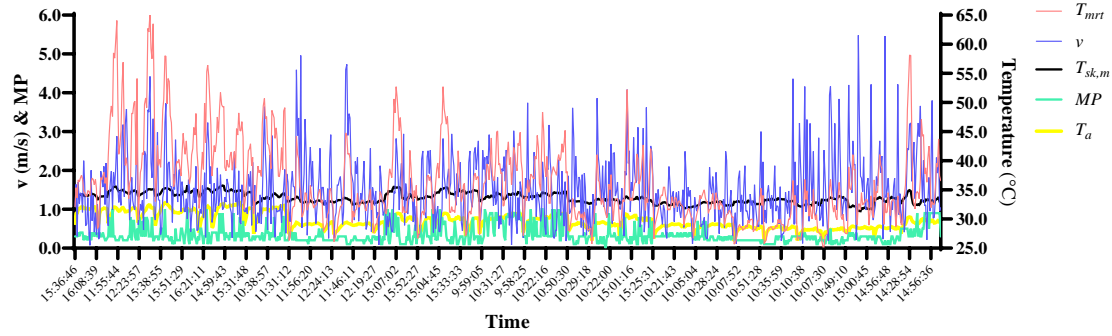
where, SVI_{mrt} is the sensed variation index of T_{mrt} (solar radiation) in each walking period and SVI_v is the sensed variation index of wind speed. The Sensed Variation Index (SVI) grades the changes in wind or solar radiation while walking in the urban continuums by integrating the coefficient of variation, which reflects the frequency of varying wind or solar radiation, and the change rate, which reflects the magnitude of varying wind and solar radiation in each walking period. SVI is sufficiently validated to describe the variations of wind or solar radiation within a short period, and the calculation of SVI can be found in Appendix B or the study conducted by Li et al. (2022b). Due to the calculation of R_DTE , a smaller R_DTE value indicates a more intensive variation in wind and solar radiation surrounding pedestrians, or a greater extent of variable thermal exposures.

3 Results

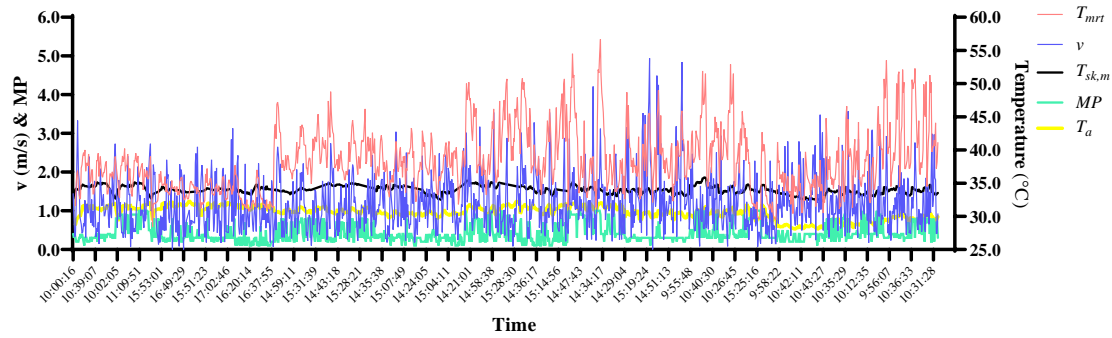
3.1 Variable thermal exposures

Despite inviting 70 subjects to attend the experiments, we obtained the valid data from only 42 of them. Because each subject completed four walking periods in a single experiment, 168 sets of walking period data were thus obtained for analysis in this study. To facilitate the observation, Figure 7 simultaneously depicts the variations of microclimate parameters around all valid walking subject, including wind speed, mean radiant temperature, and air temperature, as well as the variation of his/her mean skin temperature and mixed thermal perception, during each walking period on campus and in the urban streets. The abscissa shows the walking period for each subject in order. Among these variables, T_{mrt} (red line) and v (blue line) exhibit much more intense fluctuations, confirming the variable thermal exposures in urban continuums characterized by fluctuating wind and solar radiation. The concurrent fluctuations of MP and $T_{sk,m}$ show that the subjects' thermal perceptions and thermo-regulation processes are sensitive

to thermal environmental stimulations. Therefore, the laws of thermal comfort while walking in these variable thermal exposures are likely to differ from those in a steady state, which deserves further investigations.



a)



b)

Figure 7 Variations of microclimate parameters, mean skin temperature and the mixed thermal perception during walking in each experiment on a) campus and in b) the urban streets

3.2 Physiological responses under variable thermal exposures

Figure 8 depicts the distribution of subjects' local sweating rates calculated in each walking period, grouped by gender and the average air temperature $\overline{T_a}$. It is seen that subjects' sweating rates of measured sites increase with the air temperature except that of the calf. The back's sweating rate range calculated in this study is between 0.4 and 0.8 mg/cm²·min, which is comparable to that of a biking person under the air temperature of 32.5±0.8°C (Morris et al.,

2013). As the $\overline{T_a}$ during walking is from 28.0 °C to 30.0°C, the average whole-body sweating rates are about 0.51 mg/cm²·min and 0.76 mg/cm²·min, respectively for females and males, while those increase to 1.04 mg/cm²·min and 1.29 mg/cm²·min at 30.0≤ $\overline{T_a}$ ≤33.0°C.

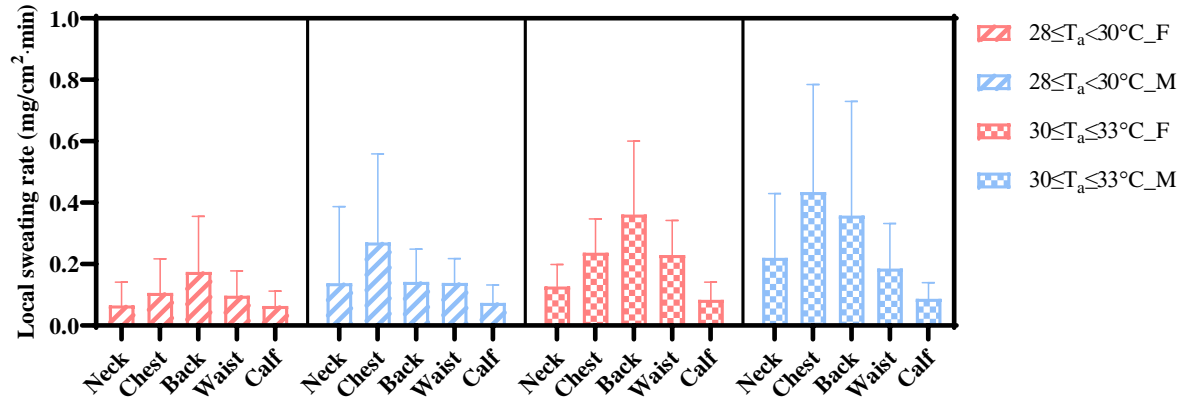
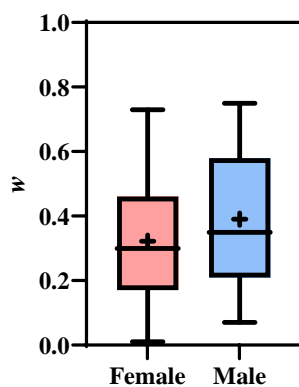
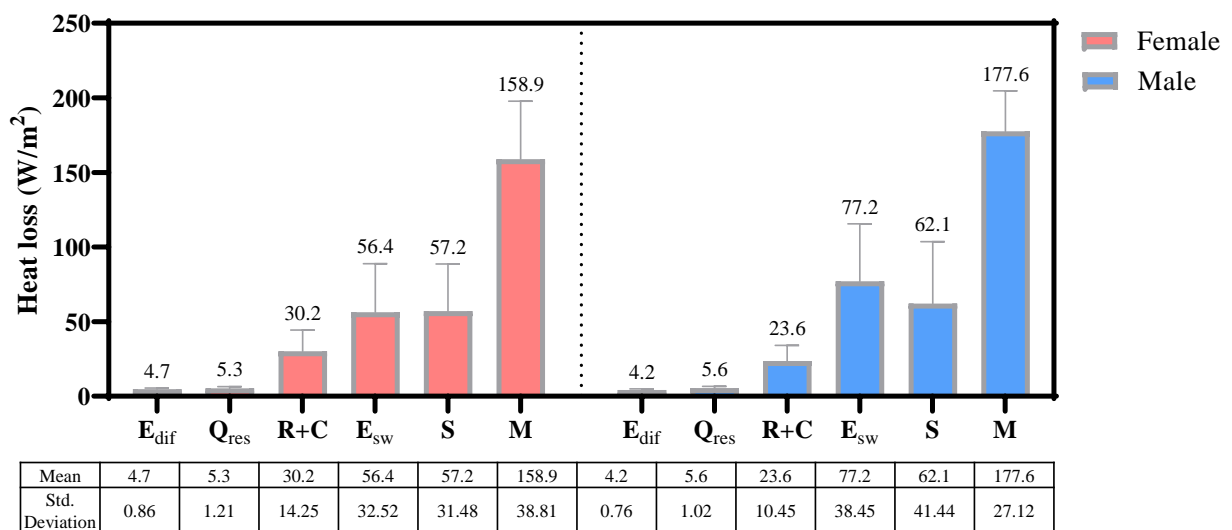


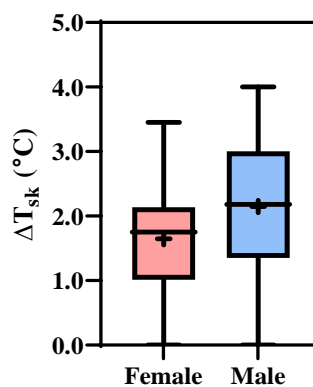
Figure 8 Local sweating rates calculated in each walking period, grouped by gender and average air temperature in each walking period.

The heat exchange between a walking human body and the variable ambient was calculated for each walking period based on the total sweating rate and other measured physiological responses. Figure 9a displays the distribution of calculated heat exchanges for all valid subjects. The heat generated (metabolic rate M in Figure 9a) by female subjects while walking is about 158.9 ± 38.8 W/m², which is smaller than the male subjects' rate of 177.6 ± 27.1 W/m². The evaporative heat loss from sweat is dominant, taking up 35%-43% of the generated heat, and male subjects have greater latent heat loss but smaller sensible heat loss than female subjects, which might be attributed to male subjects' higher sweating rate and a reduced skin temperature caused by evaporative heat loss. A notable heat storage that takes up about 35.0% of the generated heat is observed, revealing the average heat stress of a walking person being exposed to variable microclimates in hot days.

In addition to the heat exchange, the traditional physiological responses that reflect the heat stress, including the skin wettedness (w) and the deviation of mean skin temperature from that of thermal neutrality (ΔT_{sk}) which was calculated from Eq. (A14-A15), are observed in Figure 9b and Figure 9c. From Figure 9b, the w of female subjects during walking is about 0.3 ± 0.2 , and that of male subjects is about 0.4 ± 0.2 . If we take the w value of 0.3 as the upper limit of thermal comfort (Shapiro et al., 1995), subjects in this study mostly have uncomfortable biased skin wettedness. From Figure 9c, ΔT_{sk} of female subjects is about $1.65 \pm 0.88^\circ\text{C}$, and that of male subjects is about $2.15 \pm 0.98^\circ\text{C}$, demonstrating a certain deviation of the thermal state from the thermal neutrality.



b)



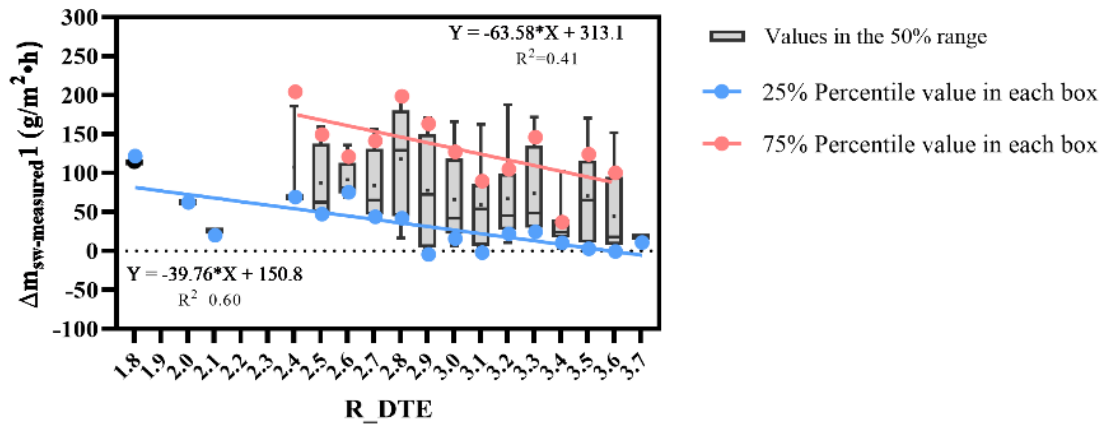
c)

Figure 9. Physiological responses of subjects during walking under variable thermal exposures: a) average heat exchange; b) average skin wettedness; c) average deviation of mean skin temperature from that of thermal neutrality

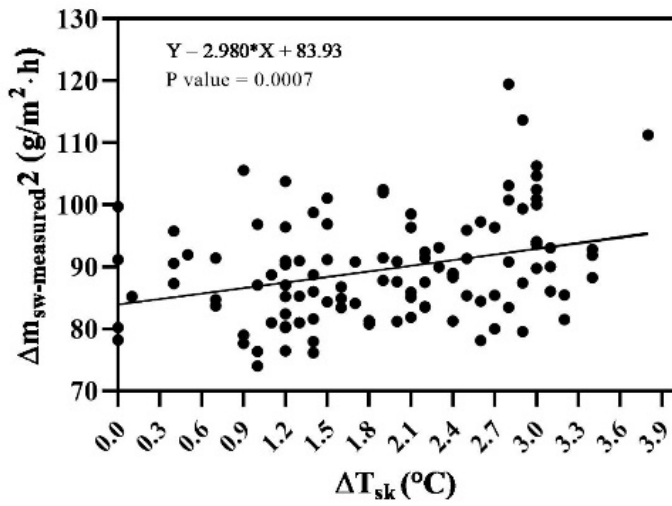
3.3 The relationship between variable thermal exposures and sweating rate

Sweating rate in the steady-state thermal environment is a linear function of the bias of metabolic rate from that under sitting still (ΔM) and ΔT_{sk} , as shown in Eq. (12). To examine if the sweating rate in this study is resulted from unsteady and variable thermal exposures, the relationship among $m_{sw_measured}$, ΔM , ΔT_{sk} , and R_DTE calculated in each walking period is analyzed in this study. For each walking period, ΔT_{sk} is the difference between averaged mean skin temperatures in this period and the neutral skin temperature, and ΔM is the difference between the calculated M and the resting metabolic rate of 58 W/m². The coefficient value of ΔM for determining the sweating rate is assumed to be the same as 0.63 in Eq. (12), which is to ensure the theoretical influence of ΔM on the sweating rate.

Therefore, the difference between $m_{sw_measured}$ and $0.63\Delta M$, named as $\Delta m_{sw_measured}1$, was assumed to be caused by R_DTE , and the $\Delta m_{sw_measured}1$ values against R_DTE values rounded to 0.1 is shown in Figure 10a. When extracting the 25% percentile and 75% percentile values in each $\Delta m_{sw_measured}1$ box and conducting the linear regression analysis between these values and R_DTE values, a negative correlation between $\Delta m_{sw_measured}1$ and R_DTE is found significant. The result demonstrates that a greater extent of variable thermal exposures (a smaller R_DTE value) leads to a higher sweating rate, while as R_DTE increases or the extent of variable thermal exposures becomes weak, $\Delta m_{sw_measured}1$ drops to a value which is supposed to be only depending on the ΔM and ΔT_{sk} .



a)



b)

Figure 10 Examining the impacts of a) R_DTE and b) ΔT_{sk} on the sweating rate in this study.

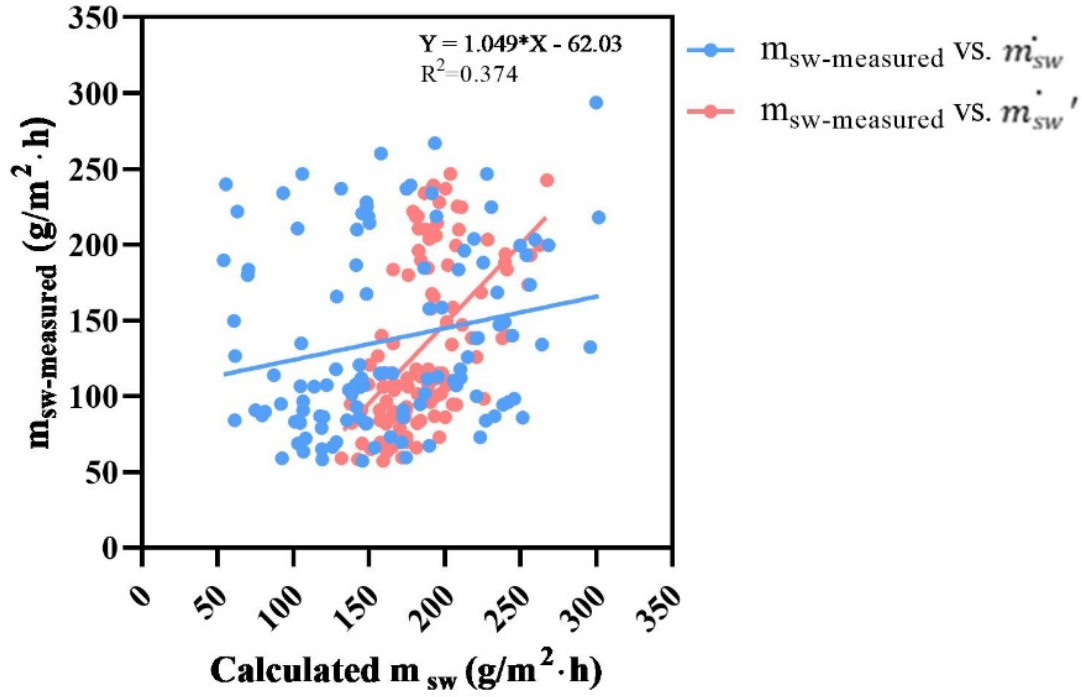


Figure 11 Comparison between the sweating rate obtained from the on-site measurement and those calculated using Eq. (12) and Eq. (23).

When relating the difference between 25% percentile and 75% percentile of $\Delta m_{sw_measured}1$ values, known as $\Delta m_{sw_measured}2$, to the ΔT_{sk} (Figure 10b), ΔT_{sk} interprets very limited $\Delta m_{sw_measured}2$ values regardless of a significant and positive linear relationship between $\Delta m_{sw_measured}2$ and ΔT_{sk} . Despite notable constant term found in regression analysis, sweating rate in this study is a function of ΔM , R_DTE , and ΔT_{sk} , as shown in Eq. (21), which significantly differs from the Eq. (12) found in a steady thermal environment.

$$m_{sw}' = 0.63 \times \Delta M - 39.76 \times R_DTE + 150.80 + (2.98 \times \Delta T_{sk} + 83.93) \quad (g/m^2 \cdot h) \quad (21)$$

The sweating rate (m_{sw}') calculated using Eq. (21) and that (m_{sw}) calculated using Eq. (12) are compared to $m_{sw_measured}$ in the Figure 11 and the equation in the figure indicates the relationship between m_{sw}' and $m_{sw_measured}$. It is obvious that m_{sw}' is much closer to

$m_{sw_measured}$ than \dot{m}_{sw} . Because the same coefficient of ΔM is used to calculate \dot{m}_{sw}' and \dot{m}_{sw} , as well as the very small coefficient of ΔT_{sk} in the Eq. (22), the difference between \dot{m}_{sw}' and \dot{m}_{sw} is primarily caused by R_DTE , demonstrating that R_DTE is more effective than ΔT_{sk} in predicting thermo-regulation process and reflecting the heat stress in dynamic thermal conditions (walking in variable thermal exposures). The result, illustrated from the derivation of R_DTE (Eq. 20), is possibly attributed to R_DTE indicating the real dynamic thermal stress by the skin temperature variability as a result of variable thermal exposures, while a ΔT_{sk} that determined by an averaged mean skin temperature during variable thermal exposures cannot.

3.4 Overall walking thermal comfort in variable thermal exposures

This section investigates how variable thermal exposures and skin wettedness during a walking period simultaneously affect the overall walking thermal comfort. For each walking period, a subject experienced one R_DTE indicating the extent of variable thermal exposures during walking, produced one skin wettedness (w), and expressed several mixed thermal perceptions (MPs). Accordingly, Figure 12 displays each subject's average MPs against his/her experienced R_DTE in each walking period, grouped by their skin wettedness. Worth noted is that the averaged MPs in one walking period represents the overall walking thermal comfort in this study. The regression line was made for average MPs and R_DTE values to display their relationship. The bubble size indicates the number of mixed thermal perceptions answered in each walking period.

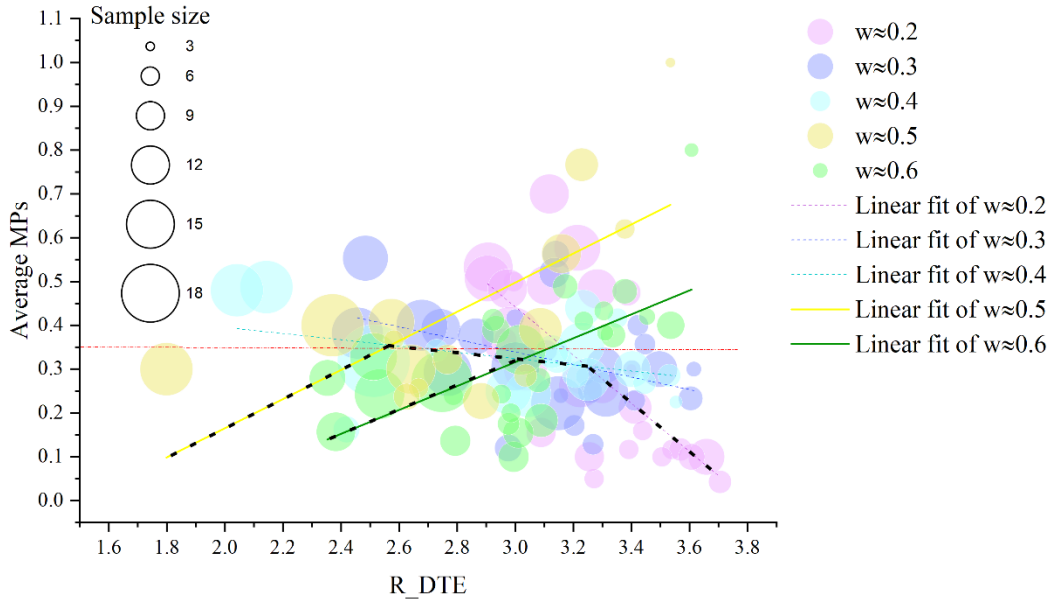


Figure 12. Average *MPs* against *R_DTE* for each subject in each walking period, grouped by subjects' skin wettedness

From Figure 12, if the w is smaller than 0.5, average *MPs* increases with the drop in *R_DTE* value. The result indicates that if the body thermo-regulation process or the body adaptation mechanism is relatively weak (little sweating with w of around 0.2 or 0.3), a greater extent of variable thermal exposures instead makes overall walking thermal perception bias uncomfortable, which might be caused by the undesired disruption of heat balance by heat gain from highly variable solar radiation or convective heat loss from highly variable wind. If the thermo-regulation process is moderate (sweating with w of greater than 0.3 but lower than or equal to 0.4), the change in average *MPs* against *R_DTE* becomes flat, which should be interpreted as highly variable wind during walking boosting the evaporative and convective cooling effects and thus neutralizing the heat gain from variable solar radiation.

What's interesting is that if the w is greater than or equal to 0.5, the average *MPs* increases with the increasing *R_DTE* value, demonstrating that if the thermo-regulation process is

intensive and indicating uncomfortable heat stress, subjects prefer a greater extent of variable thermal exposures. It is believed that alliesthesia appears under cooling effects brought by amplified downward changes in solar radiation and upward changes in wind speed. This phenomenon continuously affects the mixed thermal perceptions, resulting in the reduced average *MPs* and comfortable biased walking experience.

4. Discussion

This study fills a research gap by evaluating walking thermal comfort while taking into account the effects of variable thermal exposures in urban continuums. It also reveals the sweating rate and heat exchange processes during outdoor walking for the first time, laying the groundwork for future studies modeling walking thermal comfort and designing sidewalks. However, such a thermal comfort study under unsteady thermal conditions needs the adoption of some assumptions and algorithms to simplify the discussed problem, thus introducing possible inaccuracies that are worthy of discussion and further refinement.

More in detail, the length of sub-route selected in Section 2.1 is to ensure each walking period is greater than 5 minutes but less than 10 minutes. Its purpose is to minimize the inaccuracy caused by using absorbent to collect sweat while walking, despite the fact that the duration for stacking the absorbent on the skin is still debated in the literature (usually more than 5 minutes) (Morris et al., 2013). Since the limited method for studying the sweating rate, especially during walking, the TA method cannot detect the dynamic changes in sweat, leading to a lack of understanding of how sweating is related to time in addition to the air temperature. Nonetheless, the critical time of sweating, according to the findings of this study, is within the time spent on each walking on hot days.

In terms of the experiment process, subjects were required to rest for 10 minutes at the end of each walking period. Table 3 displays the *TSV*, heart rate, and mean skin temperature before

starting the next walking period. Due to the thermal states after rests approaching neutrality and the negligible sweating rate of $0.015 \text{ mg/cm}^2\cdot\text{min}$ calculated by Eqs. (A13-A14), we assume that each walking period starts without heat stress. However, the deviation of each variable in the Table 3 demonstrates that individual differences may cause some inaccuracies. Besides, as shown in Table 3, the average MP , sweating rate, and mean skin temperature in each walking period are not significantly related to the order of the walking periods, demonstrating that thermal adaptation of a single subject who completes 4 times of walking and resting in one experiment may not significantly influence the subjects' physiological responses. In view of this, the findings in this study particularly applies to the appraisal of around 10 minutes' outdoor walking thermal comfort, whereas the evaluation of long-term walking thermal comfort relies on more advanced and more portable devices for measuring sweating rate and heat exchanges.

Table 3. Distribution of TSV , RH , and $T_{sk,m}$ during the rest and the impacts of walking route order on the MP , $T_{sk,m}$, and $m_{sw_measured}$ during walking.

Descriptive statistics	HR	TSV	$T_{sk,m}$
Minimum	60.00	-2.40	30.76
Maximum	106.0	2.40	35.31
Range	46.00	4.80	4.55
Mean	77.78	0.37	33.70
Std. Deviation	12.66	0.91	0.78
Std. Error of Mean	1.170	0.08	0.07
Pearson correlation	Road order vs. MP	Road order vs. $T_{sk,m}$	Road order vs. $m_{sw_measured}$
Pearson coefficient	-0.01	-0.12	0.01
R squared	0.00	0.01	0.00
P value (two-tailed)	0.86	0.15	0.88

Significant? (alpha = 0.05)	No	No	No
-----------------------------	----	----	----

Further possible sources of limitation lie in the analysis of heat exchange in Section 3.2 and the derivation of predicting sweating rate during walking in variable thermal exposures in Section 3.3. Despite the fact that Section 3.2 investigates the averaged heat exchange under variable thermal exposures on hot days, the individual differences reflected by the deviation values are notable. It is possible that some people lose heat primarily by increasing the skin temperature, while others lose heat primarily by sweating, leading to differences in the heat exchange processes. However, adapting walking thermal comfort assessment and modelling to different populations are always limited in the literature. Regarding the derivation of Eq. (22) in Section 3.4, a notable constant term is observed, and the Eq. (22) interprets around 40% of measured sweating rate ($m_{sw_measured}$) in this study. Therefore, other factors may influence the sweating rate during walking in variable thermal exposures, and on the other hand, R_DTE has potentials to be furtherly improved to reflect and predict the dynamic thermal stress in the future study.

Regarding the integrated impacts of variable thermal exposures and sweating wettedness on mixed thermal perceptions in Section 3.4, variable thermal exposures played a significant role in determining the overall walking thermal comfort, and their effects depend on the intensity of the thermo-regulation process or the body adaptation mechanism during walking. Because the extent of variable thermal exposures R_DTE was defined based on the skin temperature variability influenced by the varying solar radiation and wind speed, skin temperature variability and skin wettedness shall be taken into account in modeling dynamic walking thermal comfort in future studies. In Fig. 12, if we treated average MPs of 0.35 as the upper threshold of comfort, shown as the red line, the bubbles below it indicate that if pedestrians can

adjust variable thermal exposures represented by R_DTE values between 1.8 and 3.7 based on their skin wettedness between 0.2 to 0.6, they can have comfortable walking experience.

In the end, despite abovementioned limitations, this is a valuable study providing a reference to model and assess the walking thermal comfort under variable thermal exposures for refining the walkability assessment and opening minds to dynamic thermal comfort study. Furthermore, this study illustrates how urban designers can create and utilize variable thermal exposures in urban continuums to adjust walking thermal comfort.

5. Conclusions

This study was conducted to assess walking thermal comfort in the complex urban continuums on hot days by revealing the heat exchange between a walking body and its dynamic surroundings, as well as the physio-psychological responses under different extent of variable thermal exposures caused by walking and building environments. The following are the main conclusions.

1) Variable thermal exposures caused by walking and complex building environments are characterized by simultaneously varying wind and solar radiation. When walking on summer days with air temperatures above 28.0°C and variable thermal exposures, the male subjects have a greater sweating rate and evaporative heat loss than the female subjects; the average w of female subjects during walking is about 0.3 ± 0.2 , and that of male subjects is about 0.4 ± 0.2 ; the average ΔT_{sk} values are $1.65\pm0.88^\circ\text{C}$ and $2.15\pm0.98^\circ\text{C}$ for female and male subjects respectively; the evaporative heat loss from sweat is dominant, and heat storage takes up 36.0% of the heat produced on average.

2) The sweating rate increases with a rise in the extent of variable thermal exposures (a decrease in R_DTE), and it is a function of ΔM , R_DTE , and ΔT_{sk} , with R_DTE having a greater impact than ΔT_{sk} and reflecting the real dynamic thermal stress during walking, which differs from the traditional function developed in a steady indoor thermal environment.

3) The overall thermal comfort represented by the average mixed thermal perceptions (MPs) within a walking period is depending on R_DTE and w . Intensive variable thermal exposures brings discomfort if the w is lower than or equal to 0.4, whereas they significantly improve the thermal comfort if the w is greater than 0.4 but lower than 0.7. Providing or developing variable thermal exposures with multiple options in sidewalks can improve overall walking thermal comfort.

Acknowledgements

The work described in this paper was substantially supported by a grant from the Research Grants Council of the Hong Kong Special Administrative Region, China (Project No. T22-504/21-R) and partially supported by the Otto Poon Charitable Foundation Smart City Research Institute.

Appendix A

Supplementary formulas used to calculate the heat exchange in Section 2.3.1

The metabolic rate in is calculated from Eq. (A1):

$$M = \left(\frac{MWC - M_0}{HR_{max} - HR_0} (HR_{wm} - HR_0) + M_0 \right) / A_b \quad (A1)$$

where, MWC is the maximal work capacity, in watts; M_0 is the resting metabolic rate, in watts; HR_{max} is the maximum heart rate during the experiment, in beats per minute (bpm); HR_0 is the heart rate at the rest collected in the preparation stage of an experiment, in bpm; HR_{wm} is the average heart rate observed in each walking period, in bpm; M is the corresponding metabolic rate, in in watts per kg or in watts.

Considering that the calculations of heat exchange are carried out per unit of body surface area, i.e., in W/m^2 , the body surface area (A_b) is given by the formula of Dubois et al. (1916) using the weight, W_b , and the height, H_b , as shown in Eq. (A2).

$$A_b = 0.007184 \times W_b^{0.425} \times H_b^{0.725} \quad (A2)$$

The estimation of MWC for different gender adopted the equations derived depending on the age, A , and the weight, W_b , in the ISO 8996 Standard (2004), as shown in Eqs. A3-A4).

$$\text{for men: } MWC = (19.45 - 0.133 \times A) \times W_{b,m} \quad (W) \quad (A3)$$

$$\text{for women: } MWC = (17.51 - 0.150 \times A) \times W_{b,w} \quad (W) \quad (A4)$$

The resting metabolic rate (M_0) would correspond to approximately 1.4 times the basal metabolism (M_b) according to Garg et al and the report of the World Health Organization (2001). The estimation of basal metabolism was based on the formulas quoted from Mifflin et al. (1990) (Eqs. A5-A7).

$$\text{for men: } M_{b,m} = 0.2 + 0.484 \times W_b + 0.303 \times H_b - 0.238 \times A \quad (W) \quad (A5)$$

$$\text{for women: } M_{b,w} = M_{b,m} - 8 \quad (W) \quad (A6)$$

$$M_0 = 1.4 \times M_{b,m} \quad (M_{b,w}) \quad (A7)$$

The estimation of maximum heart rate (HR_{max}) was determined by the formula ($208-0.7 \times A$) with a standard deviation of 11 bpm. The heart rate of rest (HR_0) was obtained from the experiments when subjects were sitting in an outdoor shade area and preparing for the experiments. The average heart rate HR_{wm} was determined using collected heart rate in each walking period during experiments.

The sensitive heat loss was calculated by Eq. (A8) with operative temperature calculated using Eq. (A9).

$$C + R = (MST - T_o) / (R_{cl} + \frac{1}{f_{cl}h}) \quad (A8)$$

$$T_o = (h_r T_{mrt} + h_c T_a) / (h_r + h_c) \quad (A9)$$

where MST presents the mean skin temperature; T_o is the operative temperature; T_{mrt} is the mean radiant temperature; T_a is the air temperature. The convective heat transfer coefficient h_c was based on the Eq. (A10) which takes into account the impacts of wind turbulence intensity on convective heat transfer (Yu et al., 2020).

$$h_c = 9.93u^{0.54} \times (1 + 1.03 \times TI \times u^{0.5}) \quad (A10)$$

where TI is the wind turbulence calculated using Eq. (A11).

$$TI = \frac{sd}{u} \quad (A11)$$

where u is the mean value of wind speed in a certain period (usually 10 minutes) and sd is the standard deviation of wind speed.

The radiative heat transfer coefficient h_r is assumed to be a constant value of 4.71 W/m²K (Xie et al., 2018). R_{cl} is the intrinsic clothing insulation in the unit of m²·K/W calculated by Eq. (A12) which was adopted from ASHRAE Handbook (2017).

$$R_{cl} = 0.155 * I_{cl} \quad (A12)$$

Where I_{cl} was assumed to be 0.36 clo in this study according to the walking shorts and short-sleeved shirt insulation introduced in ASHRAE Handbook (2017).

The sweating rate developed in the steady thermal environment can be calculated using Eq. (A13):

$$m_{sw} = 0.63[(M - W) - 58] + 50 \times \Delta t_{sk} \quad g/(m^2 \cdot h) \quad (A13)$$

where ΔT_{sk} is an skin temperature deviation from the neutral one and is calculated by Eq. (A14).

$$\Delta T_{sk} = MST - T_{sk,n} \quad ^\circ C \quad (A14)$$

where $T_{sk,n}$ is the natural skin temperature and is calculated using Eq. (A15)

$$T_{sk,n} = 33.9 - 0.69 \times \left(\frac{M}{58} - W \right) \quad (A15)$$

The maximum explorative heat loss to determine the skin wittedness is calculated by Eq. (A16):

$$E_{max} = (h_c + h_r) \cdot i_m \cdot LR \cdot (p_{sk,s} - p_a) \quad (A16)$$

where, i_m is the total vapor permeation efficiency and is set as 0.42 in calculation according to subjects' clothes (walking shorts) (ASHRAE, 2017); LR equals approximately 16.5 K/Kpa at typical indoor conditions; $p_{sk,s}$ is the water vapor pressure at skin, normally assumed to be that of saturated water vapor at skin temperature.

Appendix B

Calculation of the Sensed Variation Index (SVI)

The calculation of the *SVI* can be visualized in Figure B.

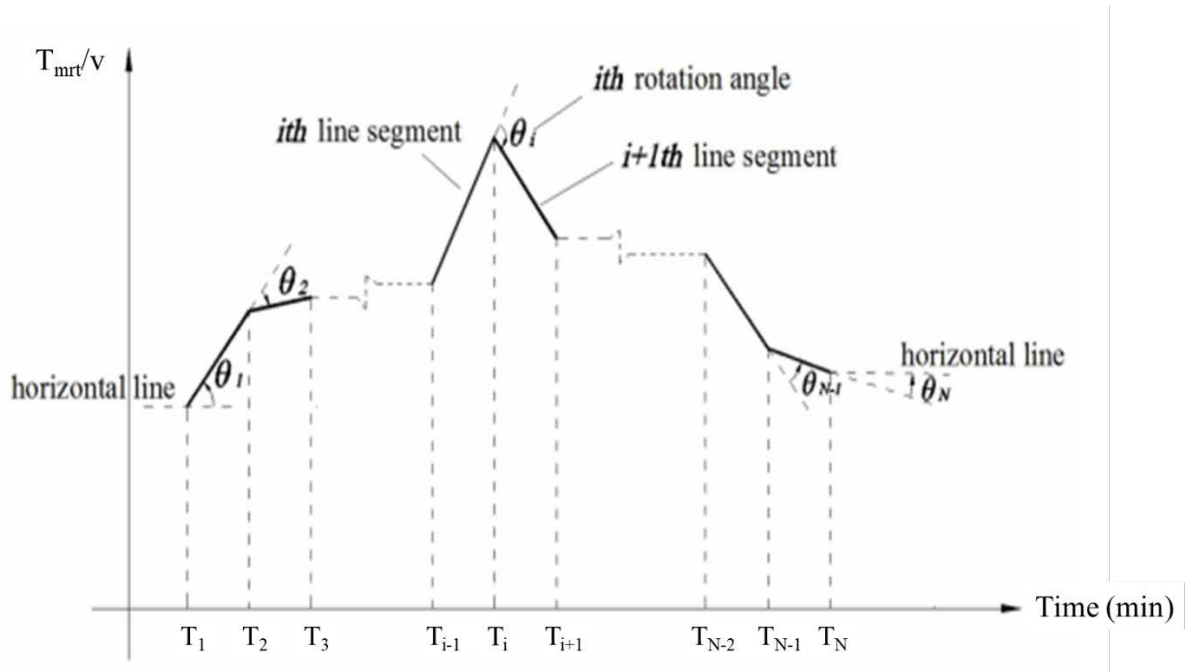


Figure B Diagram of rotation angle and line segment of a parameter's variation: The abscissa shows the total time for one walking period, and T_i shows the time corresponding to the i^{th} thermal perception. The ordinate shows the value of T_{mrt} or v .

The Sensed Variation Index (SVI) (Li et al., 2022b), which integrates the coefficient of variation and change rate of solar radiation (T_{mrt}) and wind (v) in each walking period, and can be calculated using Eq. (B1).

$$SVI = cv \times \alpha \quad (^\circ/\text{min}) \quad (\text{B1})$$

where, cv is the coefficient of variation to describe the quantitative variations including change amplitude and change frequency of T_{mrt} and v in each walking period, and can be calculated using Eq. (B2)

$$cv = \frac{\sqrt{\frac{1}{N} \sum_{i=1}^N (y(i) - \bar{y})^2}}{\bar{y}} \quad (\text{B2})$$

where $y(i)$ is the ordinate of the T_{mrt} or v corresponding to the transient answer as a polyline in the rectangular coordinate system; i is the i^{th} question answered in a walking period; the time interval between i and $i+1$ is the duration of a sequential answer; N is the total number of questionnaire surveys in a walking period; \bar{y} is the mean of the $y(i)$ values.

α in the Eq. (B1) represents the contour variation of T_{mrt} or v per minute, indicating the variation acceleration or change rate of T_{mrt} or v , and can be calculated using Eq. (B3) in the Appendix B.

$$\alpha = \frac{\sum_{i=1}^N \theta_i}{T} \quad (^\circ/\text{min}) \quad (\text{B3})$$

where T in minutes is the total period for one walking; θ_i is the rotation angle for one change in a parameter, as shown in Figure 5, and is calculated by Eqs. (B4-5)

$$\theta_i = \begin{cases} \arctan|k_i| & i = 1 \text{ or } N \\ |\arctan k_i - \arctan k_{i-1}| & 2 \leq i \leq N-1, \text{ and } k_i \times k_{i-1} \geq 0 \\ \arctan|k_i| + \arctan|k_{i-1}| & 2 \leq i \leq N-1, \text{ and } k_i \times k_{i-1} < 0 \end{cases} \quad (\text{B4})$$

$$k_i = \begin{cases} \frac{y(i+1)-y(i)}{T(i+1)-T(i)} & 1 \leq i \leq N-1 \\ \frac{y(N)-y(N-1)}{T(N)-T(N-1)} & i = N \end{cases} \quad (\text{B5})$$

When $2 \leq i \leq N-1$, θ_i is the extent of rotation between two adjacent change line segments, while when $i = 1$ or N , it is the acute angle formed by the first or N^{th} line segment and a horizontal line. When $1 \leq i \leq N-1$, k_i is the slope of the i^{th} line segment; in another word, the change rate between i^{th} parameter value and $(i-1)^{\text{th}}$ parameter value; while when $i = N$, it is the slope of $(N-1)^{\text{th}}$ line segment.

Appendix C

Calibration method of the measured T_g during movement

The author's previous work (Li et al., 2022b) has revealed the stabilized time of T_g after moving the black ball thermometer from sunlight (shade) to shade (sunlight), as shown in Figure C1, with 2 minutes assumed as the minimum stabilized time of T_g after one step change in the solar radiation. Because the calibration work was not explained in detail in the previous study, it is supplemented in this study's Appendix C.

On sunny days, if walking in a thermal condition with relatively stable solar radiation lasts more than 2 minutes, the T_g in this condition were approximated using the T_g measured before leaving the condition. Due to the frequent changes in solar radiation in this study, the time between each upward or downward change in solar radiation is typically less than 2 minutes. Based on the Figure C1, to facilitate the calibration of T_g , we assumed that the T_g changes linearly during the response time after a change in solar radiation, and that the change rate is determined by dividing the difference between the T_g right before leaving this change and the

T_g once entering this change by the duration in this change. The time of entering and leaving the change was recorded by the experiment assistant during experiments.

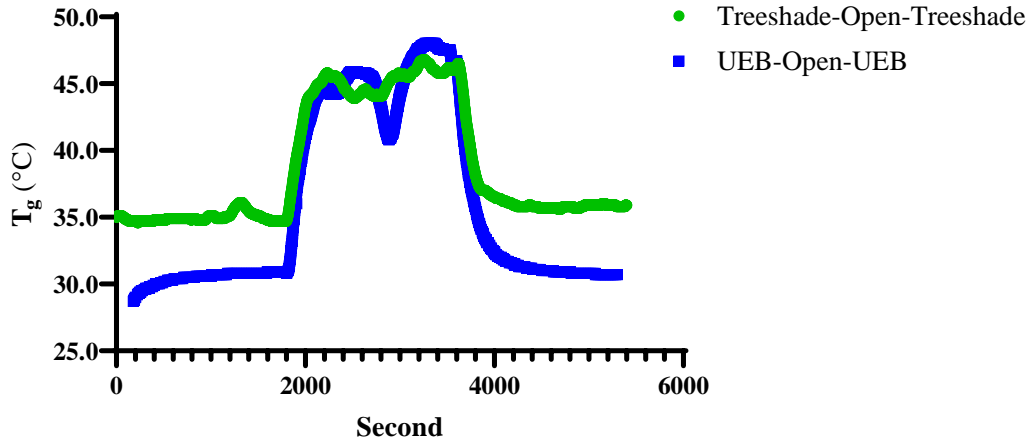


Figure C1. Variation of globe temperature from shade to sunlight and from sunlight to shade (Li et al., 2022b).

Therefore, the measured T_g after one change in the solar radiation is calibrated using the following Eqs. (C1&C2). On cloudy days, there were no intense changes in solar radiation, and the measured globe temperatures during walking were not adjusted.

$$T'_{g,change}1 = T_{g,preparation} + 120 \times \left(\frac{T_g(before\ leaving) - T_g(once\ entering)}{t} \right) \quad (C1)$$

$$T'_{g,change}(n + 1) = T'_{g,change}(n) + 120 \times \left(\frac{T_g(before\ leaving) - T_g(once\ entering)}{t} \right) \quad (n \text{ from } 1) \quad (C2)$$

where, $T'_{g,change}1$ is the first encountered change in the solar radiation after the preparation or the rest; n represents the n^{th} change in the solar radiation encountered during walking; t represents the time between two changes in the solar radiation; the number of 120 represents the stabilized time of T_g .

Figure C2 shows the measured T_g and the calibrated T_g during one walking period. It is clear that the proposed calibration method has effectively calibrated the measured T_g after taking into account the response time. Nevertheless, the method should be used with caution since it was proposed with the assumption that the stabilized time of T_g is 2 minutes.

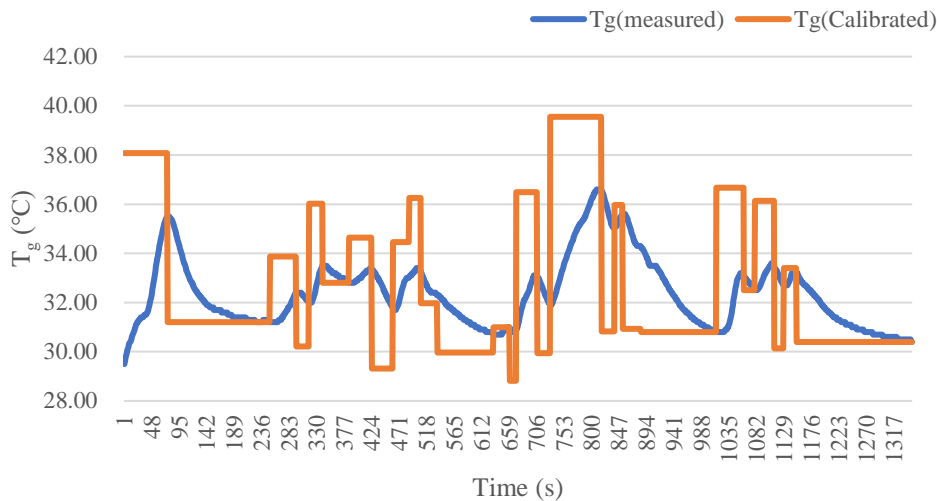


Figure C2. The variation of measured T_g and calibrated T_g during one walking period.

6. Reference

- ASHRAE. (2017). Chapter 9, ASHRAE Handbook—Fundamentals. In. Atlanta.
- Arens, E., Zhang, H., & Huizenga, C. (2006). Partial-and whole-body thermal sensation and comfort—Part II: Non-uniform environmental conditions. *Journal of thermal Biology*, 31(1-2), 60-66.
- Bravata, D. M., Smith-Spangler, C., Sundaram, V., and et al. (2007). Using pedometers to increase physical activity and improve health: a systematic review. *Jama*, 298(19), 2296-2304.
- Bröde, P., Fiala, D., Blazejczyk, K., and et al. (2009). Calculating UTCI equivalent temperature. *Environmental Ergonomics XIII, University of Wollongong, Wollongong*, 49-53.
- Bröde, P., Fiala, D., Błażejczyk, K., and et al. (2012). Deriving the operational procedure for the Universal Thermal Climate Index (UTCI). *International journal of biometeorology*, 56(3), 481-494.
- Candas, V., Libert, J., & Vogt, J. (1983). Sweating and sweat decline of resting men in hot humid environments. *European journal of applied physiology and occupational physiology*, 50(2), 223-234.
- De Dear, R. (2011). Revisiting an old hypothesis of human thermal perception: alliesthesia. *Building Research & Information*, 39(2), 108-117.
- Fiala, D., Havenith, G., Bröde, P., Kampmann, B., & Jendritzky, G. (2012). UTCI-Fiala multi-node model of human heat transfer and temperature regulation. *International journal of biometeorology*, 56(3), 429-441.

- Gagge, A., Stolwijk, J., & Nishi, Y. (1969). Prediction of Thermal comfort when thermal equilibrium is maintained by skin sweating. *ASHRAE Journal*.
- Havenith, G., Fogarty, A., Bartlett, R., Smith, C. J., & Ventenat, V. (2008). Male and female upper body sweat distribution during running measured with technical absorbents. *European journal of applied physiology*, 104(2), 245-255.
- HKO. (2020). Monthly Extract of Meteorological Observations, 2020 (Publication no. <https://www.hko.gov.hk/en/cis/monthlyExtract.htm?y=2020>). from Hong Kong Observatory
- Höppe, P. R. (1999). The physiological equivalent temperature—a universal index for the biometeorological assessment of the thermal environment. *International journal of Biometeorology*, 43(2), 71-75.
- Höppe, P. R. (1993). Heat balance modelling. *Experientia*, 49(9), 741-746.
- Houdas, Y., & Ring, E. (2013). *Human body temperature: its measurement and regulation*: Springer Science & Business Media.
- ISO. (2004). Ergonomics of thermal environment-Determination of metabolic rate. In. Geneva, Switzerland: International Standard Organisation
- ISO. (2005). Ergonomics of the thermal environment—Analytical determination and interpretation of thermal comfort using calculation of the PMV and PPD indices and local thermal comfort criteria. *International Organization for Standardization: Geneva, Switzerland*.
- Jia, X., Wang, J., Zhu, Y., Ji, W., & Cao, B. (2022) Climate chamber study on thermal comfort of walking passengers at different moving speeds. *Building and Environment*, 224, 109540.
- Kärmeniemi, M., Lankila, T., Ikäheimo, T., Koivumaa-Honkanen, H., & Korpelainen, R. (2018). The built environment as a determinant of physical activity: a systematic review of longitudinal studies and natural experiments. *Annals of behavioral medicine*, 52(3), 239-251.
- Kraning, K. K., & Sturgeon, D. A. (1983). Measurement of sweating rate with capacitance sensors. *Annals of biomedical engineering*, 11(2), 131-146.
- Kubota, H., Kamata, N., Ijichi, T., Horii, T., & Mastsuo, T. (1996). Prediction of mean skin temperature as an index of human response to the thermal environment. *Proceeding of Indoor Air Quality and Climate, Nagoya, Japan*.
- Kubota, H., Yamakoshi, T., Kamata, N., Asahina, R., Hamada, H., & Wakamatsu, S. (2004). Prediction of mean skin temperature for people in hot environment considering evaporating efficiency of sweating. *Journal of Environmental Engineering(Transaction of AIJ)*(575), 83-89.
- Labdaoui, K., Mazouz, S., Moeinaddini, M., Cools, M., & Teller, J. (2021). The Street Walkability and Thermal Comfort Index (SWTCI): A new assessment tool combining street design measurements and thermal comfort. *Science of the total environment*, 795, 148663.
- Lau, K. K.-L., Shi, Y., & Ng, E. Y.-Y. (2019). Dynamic response of pedestrian thermal comfort under outdoor transient conditions. *International Journal of Biometeorology*, 63(7), 979-989.
- Lee, L. S., Cheung, P. K., Fung, C. K., & Jim, C. Y. (2020). Improving street walkability: Biometeorological assessment of artificial-partial shade structures in summer sunny conditions. *International Journal of Biometeorology*, 64(4), 547-560.
- Li, B. (2012). *Indoor thermal environment and human thermal comfort*: Chongqing University Press.

- Li, J., Niu, J., Huang, T., & Mak, C. M. (2022). Dynamic effects of frequent step changes in outdoor microclimate environments on thermal sensation and dissatisfaction of pedestrian during summer. *Sustainable Cities and Society*, 79, 103670.
- Li, J., Niu, J., & Mak, C. M. (2022b). Study of pedestrians' mixed thermal responses when experiencing rapid and simultaneous variations in sun and wind conditions in urban continuums. *Sustainable Cities and Society*, 104169.
- Liu, S., Nazarian, N., Niu, J., Hart, M., & de Dear, R. (2020). From thermal sensation to thermal affect: A multi-dimensional semantic space to assess outdoor thermal comfort. *Building and Environment*, 182, 107112.
- Lo, R. H. (2009). Walkability: what is it? *Journal of Urbanism*, 2(2), 145-166.
- Malchaire, J., ALFANO, F. R. d. A., & Palella, B. I. (2017). Evaluation of the metabolic rate based on the recording of the heart rate. *Industrial health*, 55(3), 219-232.
- Mayer, H., & Höppe, P. (1987). Thermal comfort of man in different urban environments. *Theoretical and applied climatology*, 38(1), 43-49.
- Melnikov, V., Krzhizhanovskaya, V. V., Lees, M. H., & Sloot, P. M. (2018). System dynamics of human body thermal regulation in outdoor environments. *Building and Environment*, 143, 760-769.
- Mitchell, D., Senay, L., Wyndham, C., Van Rensburg, A., Rogers, G., & Strydom, N. (1976). Acclimatization in a hot, humid environment: energy exchange, body temperature, and sweating. *Journal of applied physiology*, 40(5), 768-778.
- Morris, N. B., Cramer, M. N., Hodder, S. G., Havenith, G., & Jay, O. (2013). A comparison between the technical absorbent and ventilated capsule methods for measuring local sweat rate. *Journal of applied physiology*, 114(6), 816-823.
- Oleson, K. W., Monaghan, A., Wilhelmi, O., Barlage, M., Brunsell, N., Feddema, J., . . . Steinhoff, D. (2015). Interactions between urbanization, heat stress, and climate change. *Climatic Change*, 129(3), 525-541.
- Ouameur, F., & Potvin, A. (2007). *Urban microclimates and thermal comfort in outdoor pedestrian spaces: a dynamic approach assessing thermal transients and adaptability of the users*. Paper presented at the The American Solar Energy Society conference proceedings, Cleveland.
- Potvin, A. (2000). Assessing the microclimate of urban transitional spaces. *Proceedings of Passive Low Energy Architecture*, 581-586.
- Shapiro, Y., Moran, D., Epstein, Y., Stroschein, L., & Pandolf, K. (1995). Validation and adjustment of the mathematical prediction model for human sweat rate responses to outdoor environmental conditions. *Ergonomics*, 38(5), 981-986.
- Vasilikou, C., & Nikolopoulou, M. (2020). Outdoor thermal comfort for pedestrians in movement: thermal walks in complex urban morphology. *International Journal of Biometeorology*, 64(2), 277-291.
- Wang, H., & Hu, S. (2018). Analysis on body heat losses and its effect on thermal sensation of people under moderate activities. *Building and Environment*, 142, 180-187.
- Xie, Y., Huang, T., Li, J., Liu, J., Niu, J., Mak, C. M., & Lin, Z. (2018). Evaluation of a multi-nodal thermal regulation model for assessment of outdoor thermal comfort: Sensitivity to wind speed and solar radiation. *Building and Environment*, 132, 45-56.
- Yang, X., Li, Y., Ma, G. and et al. (2005). Study on weight and height of the Chinese people and the differences between 1992 and 2002. *Zhonghua liu xing bing xue za zhi= Zhonghua liuxingbingxue zazhi*, 26(7), 489-493.
- Yao, Y., Lian, Z., Liu, W., & Shen, Q. (2008). Experimental study on physiological responses and thermal comfort under various ambient temperatures. *Physiology & Behavior*, 93(1-2), 310-321.

- Yu, Y., Liu, J., Chauhan, K., de Dear, R., & Niu, J. (2020). Experimental study on convective heat transfer coefficients for the human body exposed to turbulent wind conditions. *Building and Environment*, 169, 106533.
- Zhang, Y., Chen, H., Wang, J., & Meng, Q. (2016). Thermal comfort of people in the hot and humid area of China—impacts of season, climate, and thermal history. *Indoor air*, 26(5), 820-830.
- Zhang, Y., Zhou, X., Zheng, Z., Oladokun, M., & Fang, Z. (2020) Experimental investigation into the effects of different metabolic rates of body movement on thermal comfort. *Building and Environment*, 168, 106489.